# CHAPTER 5

# RESULTS AND DISCUSSION

## 5.1 The deceleration lens systems

The deceleration lens was tested for insulation of the Teflon insulator which is connected between the electrodes by a gigaohm meter and a power supply up to 30 kV. The deceleration lens systems were aligned in the big chamber of the 30-kV vertical bioengineering ion implanter (CMU3) by paper which was bombarded by ion beams. If the beam-burnt spot on the paper was not at the lens entrance hole, the deceleration lens system was moved in order to let the ion beam pass the hole at the top of the cover so that ion beam current can be measured by the Faraday cup with secondary electron suppressor. The shapes of ion beam and the burnt spot of the testing paper are shown in Figure 5.1.

From Figure 5.1, it is seen that the ion beam at the deceleration lens entrance has a shape of Gaussian distribution and a diameter of about 20 mm. In Figure 5.2 (b), the ion beam current was 160 nA, the bombarding time was 30 minute, and nitrogen ion ($N_2^+$) beam was used for bombardment of the paper.

**5.2 Measurement of ultra-low-ion beam energy**

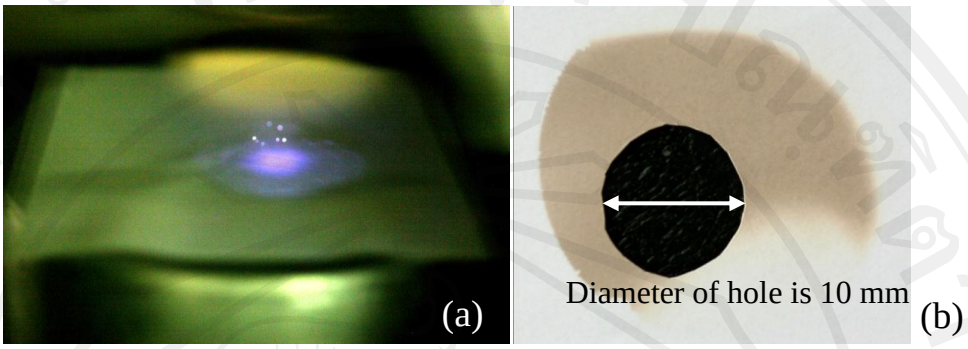


Figure 5.1. Test of the beam position at the deceleration lens for alignment of the lens. (a) Shape of ion beam. (b) Paper was burned by ion beam at the top of cover.

The deceleration lens system for measurement of the ion beam energy was installed in the big chamber of CMU3. In the measurement of the ion beam energy, it is very important to confirm the simulation of the deceleration lens by SIMION program version 8.0. The measurement of the ion beam energy used an electrostatic field for bending ion beam as the bending distance was related to the ion energy by equation 2.81 with an error of energy described by equation 2.82. Results were shown in 3 parts, the first part from theory, the second part from simulation, and the last one from experiment. The ion beam current depended on positions. Information for operation of CMU3 in the part of experiment is shown in appendix B. The experiments had 4 conditions to confirm the simulation. Each experiment had 3 steps for measurement ion beam current depending on the position. The first step was turning off the deceleration lens and the electrostatic plates, the second step was turning on the deceleration lens but turning off the electrostatic plates, and the third step was turning on both the deceleration lens and the electrostatic plates.

In the first experiment, the first simulation used the original ion beam energy of 15 keV before entering the deceleration lens, and after the ions were decelerated, the ion beam energy was 230 eV. Ions having the ion beam energy 230 eV would be bent by the electrostatic field. The first simulation is shown in Figure 3.10 (which is re-shown here). The potentials given to the electrode plates were 50 V and 0 V. The information of the first experiment is shown in Table 5.1 and the graph of ion beam currents depending on positions is shown in Figure 5.2.

In the second experiment, the original ion beam energy was 15 keV. From simulation, the energy was reduced to 56.5 eV. The potentials given to electrode plates were 12 V and 0V. The information of the second experiment is shown in Table 5.2 and the graph of ion beam currents in relation of the position is shown in Figure 5.3.

In the third experiment, the original ion beam energy was 13 keV. From simulation, the ion beam energy was reduced to 39 eV. The potentials given to electrode plates were 10 V and 0 V, respectively. The information of the third experiment is shown in Table 5.3 and the graph of ion beam currents depending on position is shown in Figure 5.4.

In the last experiment, the original ion beam energy was 10 keV. From simulation, the ion beam energy was reduced to 32 eV. The potentials given to electrode plates were 9 V and 0 V, respectively. The information of the third experiment is shown in Table 5.4 and the graph of ion beam currents depending on position is shown in Figure 5.5.

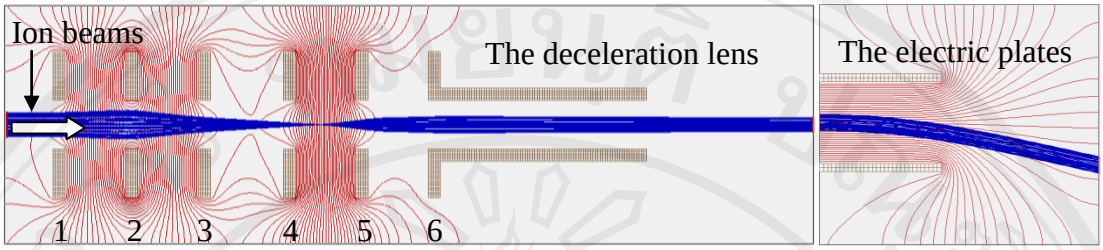


Figure 3.10. Configuration of the deceleration lens with the electric plates for bending ion beam.

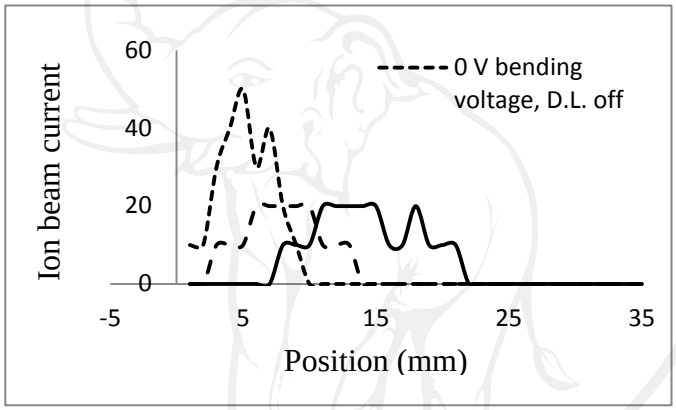


Figure 5.2. Result of the first experiment showing the dependence of ion beam current on position and the bending distance of ion beam as 8 mm.

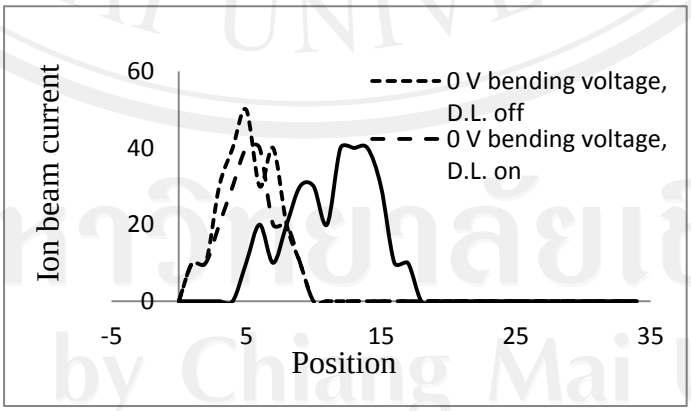


Figure 5.3. The result of the second experiment, showing the ion beam current depending on position and the bending distance of ion beam as 8 mm.

Table 5.1. Summary of fist experiment information on the measurement of the decelerated-ion energy. (a) The potential of each electrode of the deceleration lens in the simulation and experiment. (b) Information of the measurement of the ion beam energy (diameter, distance of ion beam bending, ion beam energy, and ion beam energy measurement error).

| Electrode No. | 1 | 2 | 3 | 4 | 5 | 6 |
|---|---|---|---|---|---|---|
| Simulation (V) | 0 | 11,200 | 0 | 0 | 15,270 | 15,270 |
| Experiment (V) | 0 | 11,200 | 0 | 0 | 15,270 | 15,270 |

(a)

| | Diameter of beam before enter the deceleration lens (mm) | Diameter of beam after enter the deceleration lens (mm) | Distance of ion bending (mm) | Ion beam energy (eV) | Ion beam energy error (eV) |
|---|---|---|---|---|---|
| Simulation | 10 | 12 | 9 | 230 | ±25.5 |
| Theory | - | - | 8.9 | 230 | ±26 |
| Experiment | 10 | 14 | 8 | 258 | ±32.2 |

(b)

Table 5.2. Summary of the second experiment information. (a) The potential of each electrode of the deceleration lens in the simulation and experiment. (b) Information of the measurement of the ion beam energy.

| Electrode No. | 1 | 2 | 3 | 4 | 5 | 6 |
|---|---|---|---|---|---|---|
| Experiment (V) | 0 | 10,650 | 0 | 0 | 15,417 | 15,417 |
| Simulation (V) | 0 | 10,650 | 0 | 0 | 15,420 | 15,420 |

(a)

| | Diameter of beam before enter the deceleration lens (mm) | Diameter of beam after enter the deceleration lens (mm) | Distance of ion bending (mm) | Ion beam energy (eV) | Ion beam energy error (eV) |
|---|---|---|---|---|---|
| Simulation | 10 | 12 | 9.1 | 56.5 | ±6 |
| Theory | - | - | 8.8 | 56.5 | ±6.4 |
| Experiment | 10 | 13 | 8 | 62 | ±7.7 |

(b)

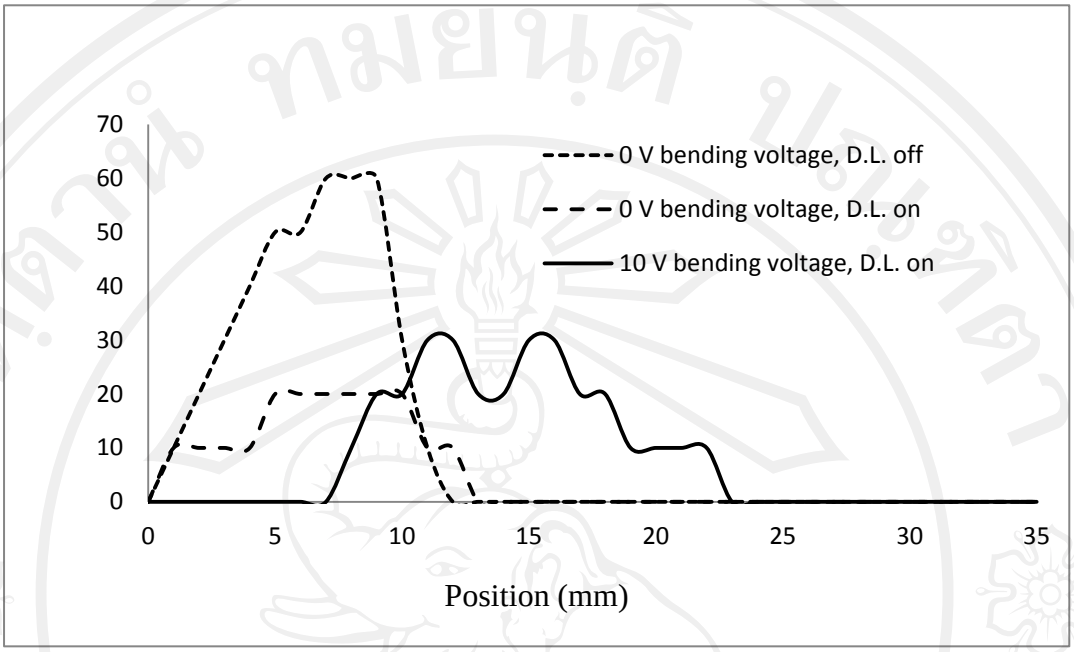


Figure 5.4. The result of the third experiment, showing the ion beam current depending on position and the bending distance of ion beam as 10 mm.

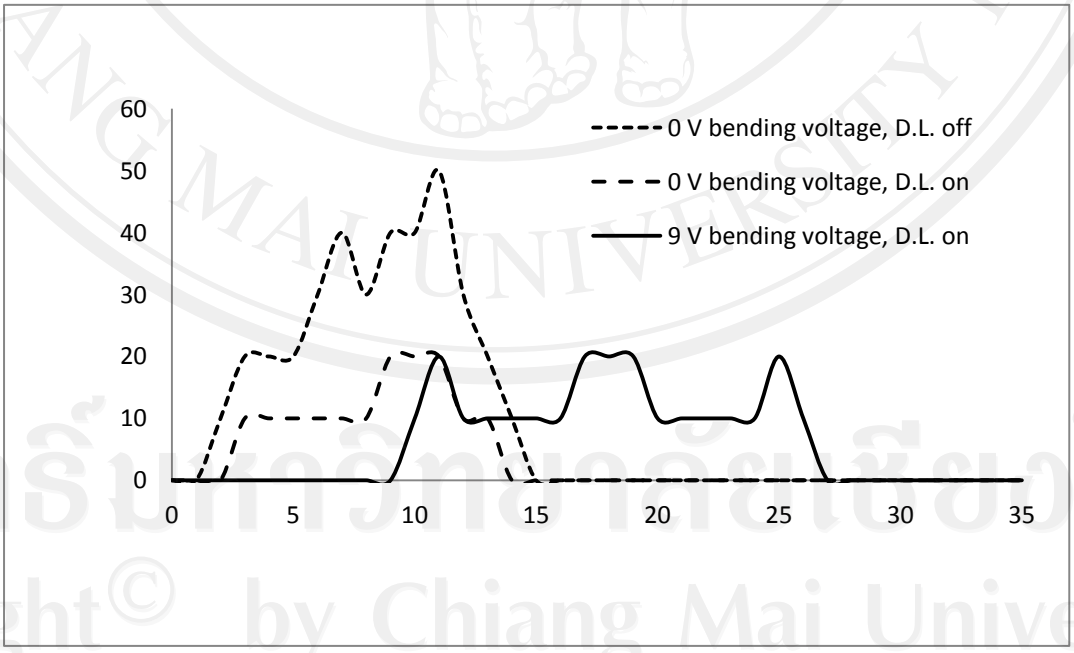


Figure 5.5. The fourth experiment result, showing the ion beam current depending on position and the bending distance of ion beam as 13 mm

Table 5.3. Summary of the third experiment result. (a) The potential of each electrode of the deceleration lens in the simulation and experiment. (b) Information of the measurement of the ion beam energy.

| Electrode No. | 1 | 2 | 3 | 4 | 5 | 6 |
|---|---|---|---|---|---|---|
| Simulation (V) | 0 | 9,100 | 0 | 0 | 13,365 | 13,365 |
| Experiment (V) | 0 | 9,100 | 0 | 0 | 13,366 | 13,366 |

(a)

| | Diameter of beam before enter the deceleration lens (mm) | Diameter of beam after enter the deceleration lens (mm) | Distance of ion bending (mm) | Ion beam energy (eV) | Ion beam energy error (eV) |
|---|---|---|---|---|---|
| Simulation | 10 | 12 | 10.6 | 39 | ±3.7 |
| Theory | - | - | 10.6 | 39 | ±3.7 |
| Experiment | 10 | 15 | 10 | 41 | ±4.1 |

(b)

Table 5.4. Summary of the fourth experiment result. (a) The potential of each electrode of the deceleration lens in the simulation and experiment. (b) Information of the measurement of the ion beam energy.

| Electrode No. | 1 | 2 | 3 | 4 | 5 | 6 |
|---|---|---|---|---|---|---|
| Simulation(V) | 0 | 7,000 | 0 | 0 | 10,280 | 10,280 |
| Experiment (V) | 0 | 7,000 | 0 | 0 | 10,275 | 10,275 |

(a)

| | Diameter of beam before enter the deceleration lens (mm) | Diameter of beam after enter the deceleration lens (mm) | Distance of ion bending (mm) | Ion beam energy (eV) | Ion beam energy error (eV) |
|---|---|---|---|---|---|
| Simulation | 10 | 10 | 11.4 | 32 | ±2.9 |
| Theory | - | - | 11.6 | 32 | ±2.8 |
| Experiment | 10 | 17 | 13 | 28.5 | ±2.2 |

(b)

The results of the measurement of ion beam energy are summarized in Table 5.5.

Table 5.5. Summary of ion beam energy and ion beam energy error calculated by simulation, theory, and measured by experiment.

| | The first experiment | The second experiment | The third experiment | The fourth experiment |
|---|---|---|---|---|
| Ion beam energy from simulation (eV) | 230.0 | 56.5 | 39.0 | 32.0 |
| Ion beam energy from theory (eV) | 230.0 | 56.5 | 39.0 | 32.0 |
| Ion beam energy from experiment (eV) | 258.0 | 62.0 | 41.0 | 28.5 |
| Ion beam energy error from simulation (eV) | ±25.5 | ±6.0 | ±3.7 | ±2.9 |
| Ion beam energy error from theory (eV) | ±26.0 | ±6.4 | ±3.7 | ±2.8 |
| Ion beam energy error from experiment (eV) | ±32.2 | ±7.7 | ±4.1 | ±2.2 |

From the experiment, the results don't same exactly with and theory and simulations, it is occurred from: the first cause is the position of ion beam not stable at different time since the limitation of the ion source, the second, the deceleration lens was aligned non-coaxial including the electrodes were not circular which it occurs the ellipticity astigmatism, the third cause is the limitation of the resolution copper's slide which the resolution copper's slide is 1 mm, and the last cause is the error of equipment including observer's error.

**5.3 Ultra-low ion energy bombardment of naked DNA**

Nitrogen ion beam ($N_2^+$) with original energy of 20 keV was decelerated to 64 eV bombarding an extracellular DNA (plasmid green fluorescence protein, pGFP) at a fluence of about $10^{15}$ ions/cm$^2$. The bombarded DNA was analyzed using gel electrophoresis and fluorometer for topological formed. A linear form was found which was identified in the bombarded DNA, as shown in Figure 5.6. The linear form was generated from the original supercoiled and relaxed forms, indicating double strand break.

Argon ion beam ($Ar^+$) with energies of 242, 304, 407, and 510 eV bombarded extracellular DNA (plasmid green fluorescence protein, pGFP) to a fluence of about $10^{15}$ ions/cm$^2$. The bombarded DNA was analyzed using gel electrophoresis and fluorometer for topological forms. Each condition had natural control and vacuum control to compare the effect of ion beam on DNA conformation

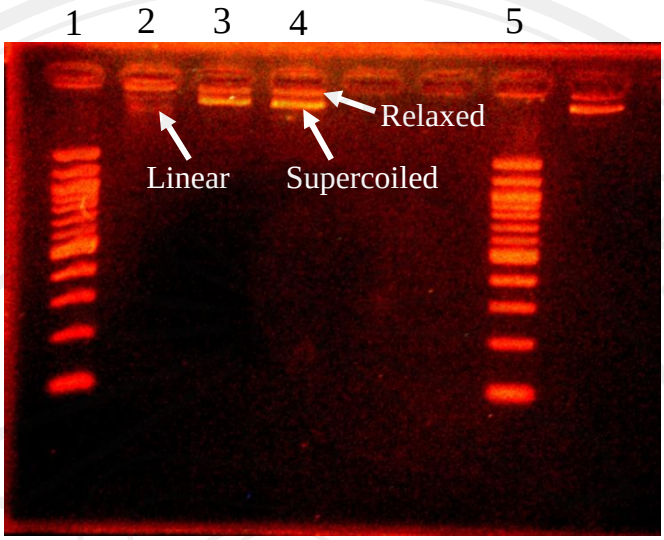


Figure 5.6. Gel electrophoresis result. Lanes 1 and 5 are markers. Lane 4 is natural control. Lane 3 is vacuum control. Lane 2 is bombarded. The DNA bands are pointed and marked by the arrows.

change and each treatment was made for 3 replications. The OriginPro8 program was used to calculate light intensity of each band. The result of treatment was compared with the natural control and vacuum control. Gel electrophoresis result of naked DNA bombarded by argon ion beam at the fluence of $10^{15}$ ions/cm$^2$ is shown in Figure 5.7. The OriginPro8 program was used to calculate light intensity of each band and to compare the results. Figure 5.8 whereas shows from the result that after Ar-ion beam bombardment relaxed form of DNA was observed while the supercoiled form decreased, but no linear form bands of DNA were observed.

It is also seen that the naked DNA bombarded by nitrogen or argon ions to the same fluence of $10^{15}$ ions/cm$^2$. It was found that N-ion bombardment could induce linear formation of DNA indicating double strand breaks whereas Ar-ion bombardment could not, even though the ion energy was relatively greater than that of

N-ions. The reason for nitrogen ion beam interaction with DNA is that nitrogen is an active element compared with inert argon. This result indicates that nitrogen ions, with energy lower than that of argon ions, are more effective in producing double strand break and damaging DNA. It seems to be conflict with common knowledge

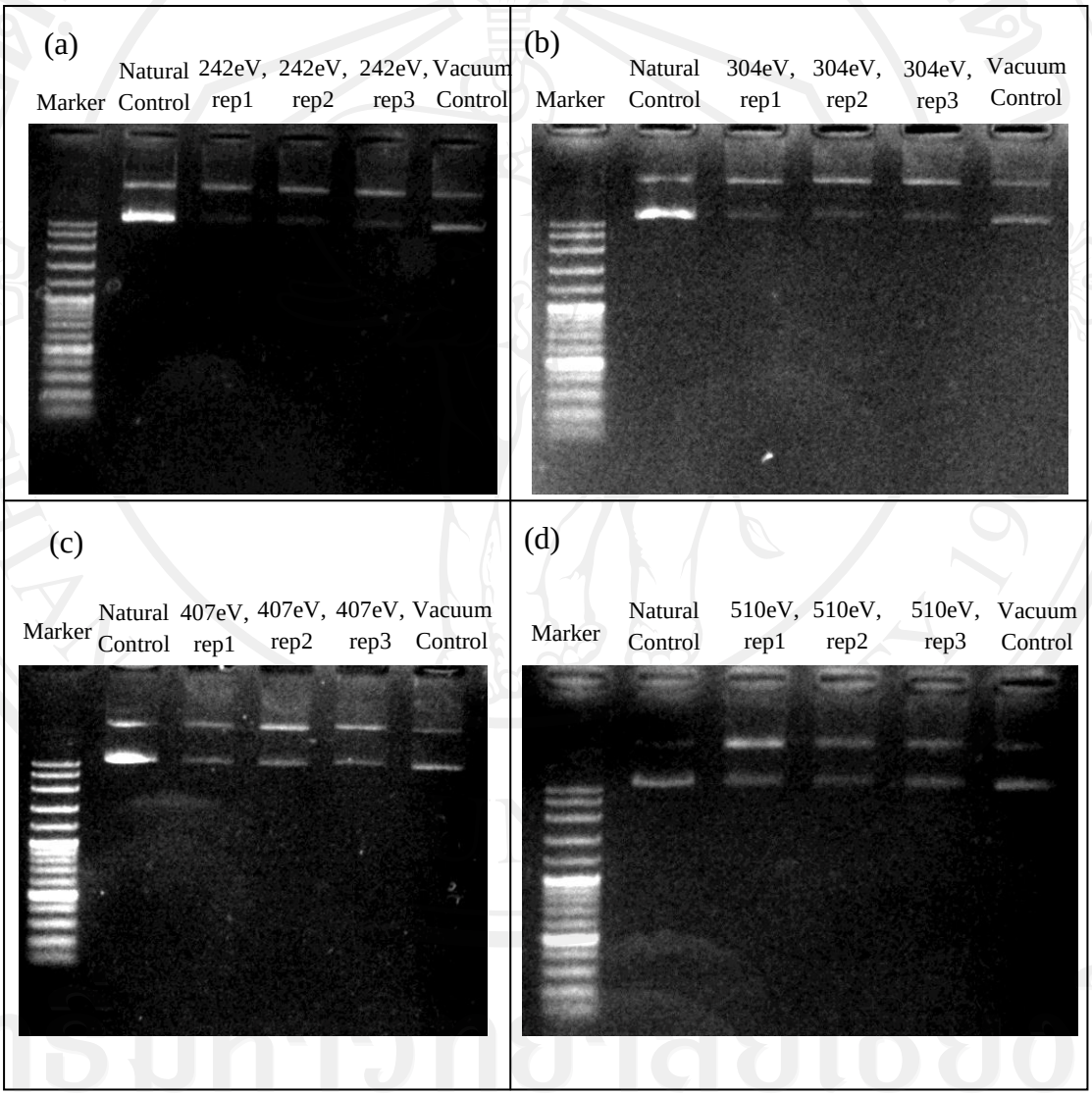


Figure 5.7. Naked DNA was bombarded by Argon ion, the fluence at $1x10^{15}$ ions/$cm^2$. (a) Ion beam energy at 242 eV, (b) at 304 eV, (c) 407 eV, and (d) 510 eV.

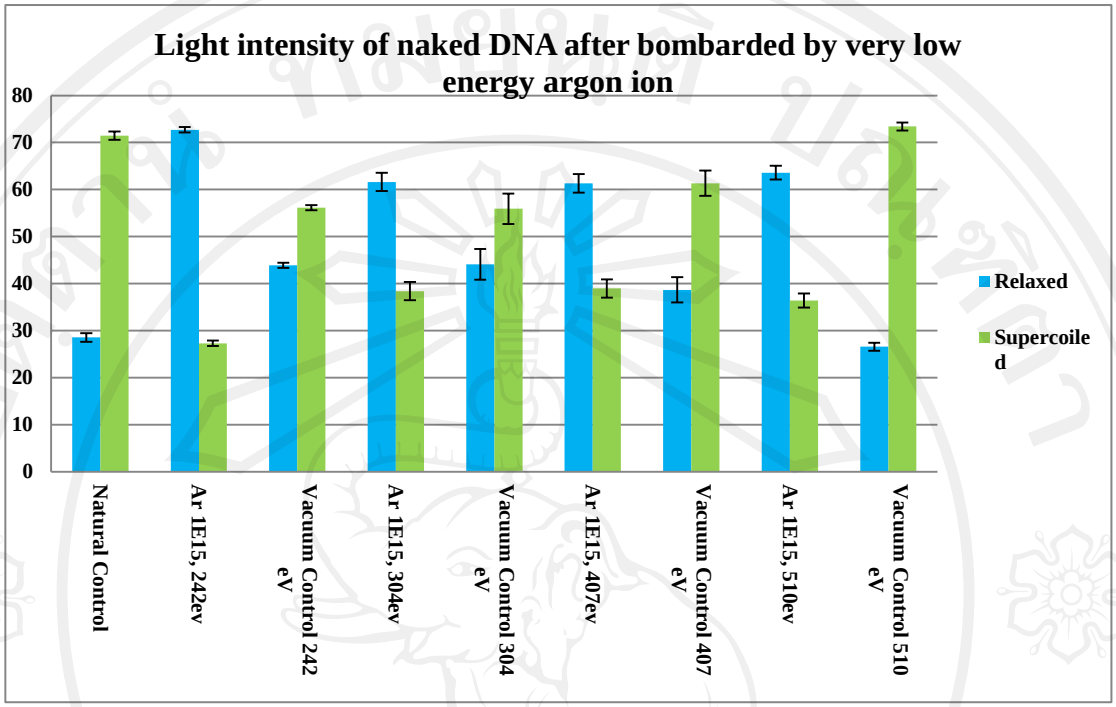


Figure 5.8. Light intensity of each DNA band calculated from the gel electrophoresis for the DNA bombarded by argon ion beam at the fluence of $10^{15}$ ions/cm$^2$ using at different energy of natural and vacuum controls.

predicting that higher energy of heavier ions able to cause more damage than lower energy of a lighter ones. Hypothesis are: the first is DNA contains much nitrogen at the nitrogenous bases, externally external introducing nitrogen will have intimate interaction with the original nitrogen and hence more effects can be observed (Yu Liangdeng et al., 2009). The second is interaction field of nitrogen ion stronger than argon ion because diameter smaller than argon. The interaction depends on inverse of distance between ion with target (ion, atom, molecule) power integer number ($1/r^n$). The interactions are: charge-charge ($1/r$), charge-dipole ($1/r^2$), dipole-dipole ($1/r^3$),

charge-induced dipole ($1/r^4$), dispersion ($1/r^6$), and repulsion interaction ($1/r^{12}$), then if small distance compare with large distance, it show that the interaction of the small distance stronger than the large distance.